

## Article

# Synergistic Effect of Carbon Nanotubes, Zinc, and Copper Oxides on Rheological Properties of Fracturing Fluid: A Comparative Study

Fatma Yehia <sup>1,2</sup>, Walaa Gado <sup>3</sup>, Abdalrahman G. Al-Gamal <sup>3</sup>, Nishu <sup>2</sup>, Chao Yang <sup>2,\*</sup>, Lihua Liu <sup>2,\*</sup> and Khalid I. Kabel <sup>3</sup>

<sup>1</sup> School of Energy Science and Technology, University of Science and Technology of China (USTC), Hefei 230026, China; fatmayehia93@outlook.com

<sup>2</sup> Guangzhou Institute of Energy Conversion, Chinese Academy of Sciences, Guangzhou 510640, China

<sup>3</sup> Egyptian Petroleum Research Institute (EPRI), Nasr City, Cairo 11765, Egypt; walaashabaan86@yahoo.com (W.G.); drkhalid1977@yahoo.com (K.I.K.)

\* Correspondence: yangchao@ms.giec.ac.cn (C.Y.); liulh@ms.giec.ac.cn (L.L.)

**Abstract:** Nanomaterials play a beneficial role in enhancing the rheological behavior of fracturing (frac) fluid by reacting with intermolecular structures. The inclusion of these materials into the fluid improves its stability, increases the viscosity of polymers, and enhances its resistance to high temperature and pressure. In this investigation, multi-walled carbon nanotubes (CNTs), nano-zinc oxides (N-ZnO), and nano-copper oxides (N-CuO) have been utilized to ameliorate the rheological properties of water-based fracturing fluid. Different concentrations of these aforementioned nanomaterials were prepared to determine their effects on the rheological behavior of the fluid. The results revealed that the size of nanoparticles ranged from 10 to 500 nm, 300 nm, and 295 nm for CNTs, N-ZnO, and N-CuO, respectively. Moreover, employing CNTs exhibited a resistance of 550 cp at 25 °C and reached 360 cp at 50 °C with a CNT concentration of 0.5 g/L. In contrast, N-CuO and N-ZnO showed a resistance of 206 cp at 25 °C and significantly decreased to 17 cp and 16 cp with higher concentrations of 10 g/L and 1 g/L, respectively. Based on these findings, this study recommends utilizing CNTs to enhance fracking fluid's chemical and physical properties, which need to be highly viscous and stable under reservoir conditions.

**Keywords:** hydraulic fracturing; frac fluid; CNTs; N-Cuo; N-ZnO; rheology



**Citation:** Yehia, F.; Gado, W.; Al-Gamal, A.G.; Nishu; Yang, C.; Liu, L.; Kabel, K.I. Synergistic Effect of Carbon Nanotubes, Zinc, and Copper Oxides on Rheological Properties of Fracturing Fluid: A Comparative Study. *Processes* **2024**, *12*, 611. <https://doi.org/10.3390/pr12030611>

Academic Editors: Qibin Li and Qingbang Meng

Received: 16 February 2024

Revised: 16 March 2024

Accepted: 17 March 2024

Published: 19 March 2024



**Copyright:** © 2024 by the authors. Licensee MDPI, Basel, Switzerland. This article is an open access article distributed under the terms and conditions of the Creative Commons Attribution (CC BY) license (<https://creativecommons.org/licenses/by/4.0/>).

## 1. Introduction

Hydraulic fracturing, or “fracking”, has emerged as an indispensable methodology in the oil and gas industry, revolutionizing energy production and playing a pivotal role in global energy supply. Fracking has drawn the attention of numerous researchers and technicians in the oil and gas industry due to its advancements in enhancing the production of oil and gas wells; increasing low-permeability reservoir production, such as from shale; providing economic benefits by improving the security of energy; reducing dependency on oil and gas imports; and being utilized in gas production as a cleaner source of energy than coal to reduce global greenhouse gas emissions [1–3]. The fracking process involves the high-pressure injection of frac fluid into underground rock formations, aiming to create fractures within oil/gas reservoirs, which enhances the production to the surface, as demonstrated in Figure 1. Therefore, a specific viscosity of the frac fluid is required to carry the proppant particles into the fractured locations [4,5].

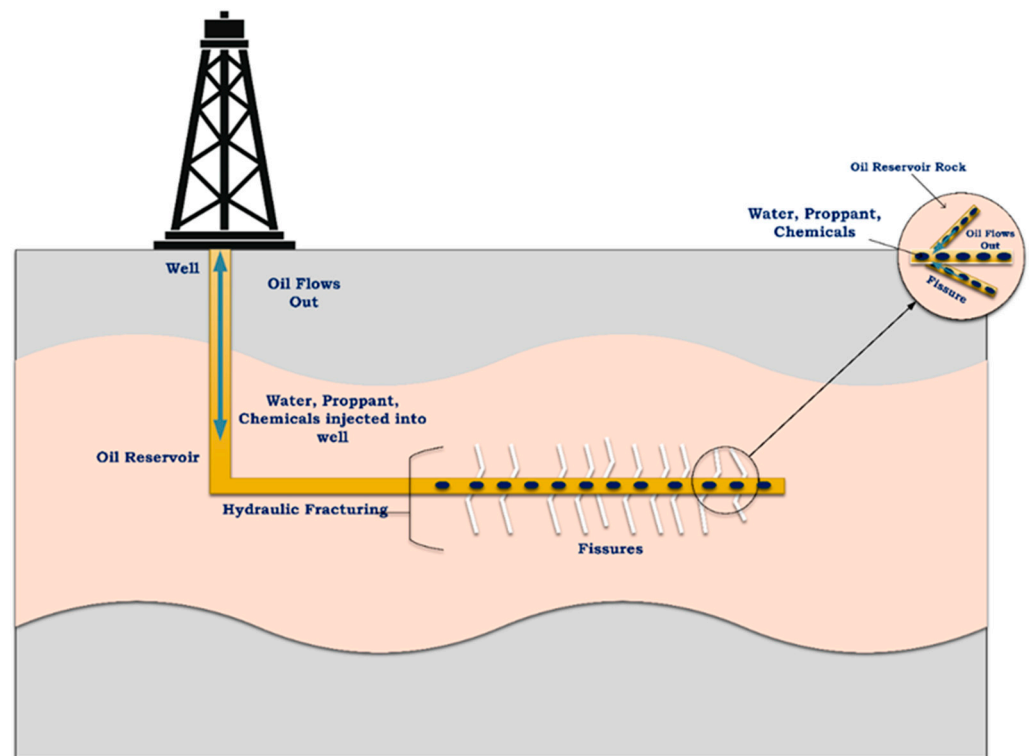


**Figure 1.** Hydraulic fracturing fluid process flow diagram for the oil reservoirs.

The selection of a frac fluid for hydraulic fracturing operations is contingent upon various considerations, including encompassing the specific type and depth of the formation, water availability and cost, and adherence to environmental regulations. In light of these considerations, different types of frac fluids have been identified, such as water-based frac fluid systems, which have become the most feasible and cost-effective option for carrying fluids, using water as the primary carrier fluid and incorporating additives like polymers, crosslinkers, biocides, and friction reducers [6]. Other types of fracking fluid systems are oil-based frac systems that utilize oil or diesel as a carrier supplemented with gels, emulsifiers, and surfactants, which are suitable for water-sensitive formations and high-temperature reservoirs [7]. Foam-based systems, which use a mixture of water, gas, and foaming agents, culminating in the generation of a dense foam capable of facilitating proppant transport and mitigating fluid loss, are preferred for low-pressure and low-permeable reservoirs [8–10]. Lastly, acid-based systems use acids such as hydrochloric or acetic acid as an essential carrier supplemented with additives such as corrosion inhibitors and iron-control agents, which are utilized for dissolving carbonate minerals and enhancing formation permeability [1].

Generally, the water-based frac fluid system is a ubiquitous choice in hydraulic fracturing operations, mainly due to its cost-effectiveness, environmental sustainability, and straightforward disposal process. To modify the fluid's properties, such as viscosity, pH, and friction reduction, to improve the performance of the fracking process, which involves creating a network of fractures in the rock formation to increase oil and gas production [1,11], and to tackle the challenges posed by the complex nature of unconventional oil and gas production and keep pace with the fast-paced advancements in hydraulic fracturing technology, scientists have initiated radical innovations in unconventional oil and gas hydraulic fracturing technology by integrating nanomaterials and technologies to meet the specific demands of hydraulic fracturing operations in various reservoir scenarios [12–16]. Nanotechnology was introduced as an innovative approach, integrating science and technology to scrutinize the individual particles in nanomaterial manufacturing and design [13,17,18]. Therefore, nanomaterials offer advantageous functionality by

providing smaller-sized particles (typically 1–100 nm). With excellent advantages over non-nano-sized substances, a small amount of nanomaterials that have a larger surface area are needed to enhance reaction activity and improve the rheological properties of frac fluids [19,20].

Two different approaches are mainly used to produce the nanomaterial: the top-down method, to synthesize nanomaterials from granular particles (bulk-material size) by reducing the size to nanoscale utilizing the physio/mechanical approaches such as ball milling, laser ablation, thermal evaporation, and sputtering; and the bottom-up method, to form the materials in the nanostructures from small atoms or molecules by employing chemical or biological techniques such as co-precipitation, chemical vapor deposition (CVD), sol-gel, and the hydrothermal method [21]. However, a top-down method is frequently used in the synthesis of nanomaterials. Moreover, among all methods, the precipitation technique has several benefits, such as ease of preparation, time savings, low-temperature requirements, energy-efficiency, and additionally has numerous options to modify the surface state of particles [22–24]. Adam et al. employed the co-precipitation method to synthesize N-ZnO particles due to its efficiency for photodegradation in the presence of low temperatures and different pH conditions [25]. In another study, Phiwdany and colleagues utilized the precipitation method to synthesize N-CuO materials using several precursors [26]. Similarly, this method was applied for N-ZnO preparation as a simple process using zinc nitrate and KOH by Pazoki et al. [27]. Figure 2 illustrates the preparation approaches for nanomaterials. Hence, nanomaterial synthesis for this study has been carried out using the top-down co-precipitation approach.

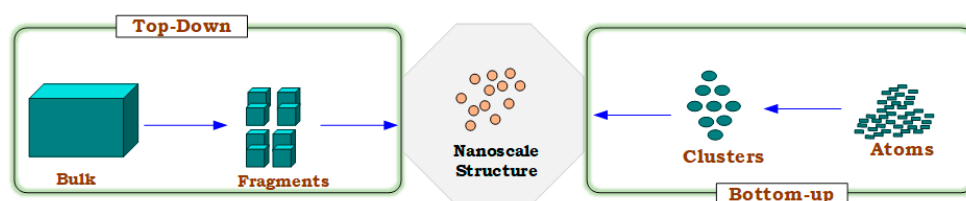


**Figure 2.** Preparation approaches for nanomaterials.

Employing nanomaterials in the oil and gas research industry has drawn tremendous interest from researchers. Khalil et al. highlighted the advancements of nanomaterials such as carbon nanotubes, metallic and metal oxide nanoparticles, and magnetic nanoparticles to improve the performance of oil and gas production processes [13], especially for improving the hydraulic frac fluid rheological properties to resist the high-pressure and high-temperature conditions of reservoirs and transport the proppants along the reservoir. Tang and colleagues utilized amino-modified multi-wall carbon nanotubes (CNTs-NH<sub>2</sub>) integrated with primary polymer fluid to enhance the rheological properties of fracking fluid. The results showed enhancement in the viscoelasticity, shear resistance, and temperature of the polymeric nano-solutions. Additionally, the use of CNTs-NH<sub>2</sub> rehabilitated the wettability of the reservoir rock, leading to changes in fluid flow and distribution within the reservoir [28]. In another study, CNTs, nano-silica, and glass beads were employed to improve the rheological characteristics of water-based drilling fluids. This study demonstrated that using the multi-walled CNTs provided a 38% coefficient of friction reduction for drilling fluid [29]. Alkalbani et al. investigated the influence of N-ZnO on the water-based mud (WBM) rheological properties from surface to downhole conditions. This study revealed that utilizing N-ZnO improved the rheological properties of WBM significantly, by 40–65% [30]. The prepared N-CuO fluid was investigated to enhance the rheological characteristics of WBM dispersed in a solution of chia seeds [31].

As mentioned in the previous studies, several research works have been performed using different nanomaterials to improve the drilling fluid or other types of fracking systems, such as guar gum systems. However, few studies focused separately on the employment of CNTs [29], N-ZnO [32], and N-CuO [33] with other nanoparticles to evaluate their effect to enhance the rheological properties of water-based fluid systems' performance

under reservoir conditions. This study focuses on exploring and evaluating the implications of a water-based fracking system for the purpose of enhancing fracking process efficacy in terms of the rheological properties of frac fluid by comparing the effects of three types of nanomaterials on the rheological properties. Therefore, in this research work, three different types of nanomaterials (CNTs, N-ZnO, and N-CuO) were selected. In addition to CNTs, the synthesis of N-CuO and N-ZnO particles by employing the precipitation approach was undertaken, and the preparation of fracking fluid was investigated. The main objective of this research work is to investigate the effect of nanomaterials on the rheological properties of the hydraulic frac fluid. The morphology, distribution, and grain size for nanomaterials were determined using high-resolution transmission electron microscopy (HR-TEM) and dynamic light scattering (DLS). Furthermore, the rheological properties of the prepared fracking fluid are evaluated and compared in the presence of different temperatures for the four samples.

## 2. Materials and Methods

### 2.1. Materials

The chemicals utilized to prepare the frac fluid were: guar gum as a gelling agent, potassium chloride (KCL, 99.9%), borax (sodium tetraborate decahydrate, 99.5%) as a crosslinker, breaker (ammonium persulphate, 98.0%), NP9 and Tween20 as a surfactant to increase the fluid viscosity, sodium hydroxide (99.5%) as pH adjusting agent, ethylene glycol (62.07 g/mol) as scale inhibitor, zinc acetate dihydrate ( $\text{Zn}(\text{CH}_3\text{COO})_2 \cdot 2\text{H}_2\text{O}$ , 99.9%), copper (II) acetate monohydrate ( $\text{Cu}(\text{CH}_3\text{COO}) \cdot \text{H}_2\text{O}$ , 99.6%), methanol (MeOH, 99.8%), ammonium hydroxide ( $\text{NH}_4\text{OH}$ , 99.9%), supplied by Sigma Aldrich; proppant from SEPPE Technologies Co., Ltd, Zhengzhou, China. Regarding the nanomaterials, CNTs were supplied by EPRI Nanotechnology Centre and N-CuO and N-ZnO were prepared at the laboratory, using quantities and equipment illustrated in Tables 1 and 2, respectively.

**Table 1.** Quantities of materials used for experimental work.

| Chemicals                               | Additive Purposes | Weight |
|---|-------------------|--------|
| Synthesis of Nano-Zinc Oxides           |                   |        |
| Zinc acetate dihydrate                  |                   | 13 g   |
| Methanol                                |                   | 100 mL |
| Ammonium hydroxide                      |                   | 5 mL   |
| Synthesis of Copper Oxide Nanoparticles |                   |        |
| Copper (II) acetate monohydrate         |                   | 2.5 g  |
| Methanol                                |                   | 20 mL  |
| Fracking Fluid Preparation              |                   |        |
| Distilled water                         |                   | 1 L    |
| Potassium chloride                      | Brine carrier     | 40 g   |
| Guar gum                                | Thickener         | 4.2 g  |
| Tween or NP9                            | Surfactant        | 1 mL   |
| CNTs                                    |                   | 0.5 g  |
| CuO nanoparticles                       |                   | 10 g   |
| ZnO nanoparticles                       |                   | 1 g    |
| Ammonium persulphate                    | Breaker           | 4 mL   |
| Borex                                   | Crosslinker       | 3 mL   |
| Sodium hydroxide                        | pH adjuster       | 4 mL   |

**Table 2.** Instruments and equipment utilized in the experimental work.

| Instruments/Equipment                                     | Purpose   |
|---|---|
| Magnetic hot plate stirrer                                | Preparation of nanomaterials and the concentrations of additives for frac fluid |
| Vacuum distillation system                                | To evaporate solvent  |
| Ball mill   | To reach the nano-size of prepared nanomaterials                                |
| Blender [Mixer]   | Preparation of fracking fluid   |
| High-resolution transmission electron microscopy (HR-TEM) | Characterization of nanomaterials   |
| Dynamic light scattering (DLS)                            |   |
| Anton Paar MCR 502 rheometer                              | Evaluation of the rheological behaviors of frac fluid                           |

### 2.2. Synthesis of Nano-Zinc Oxides

The nano-zinc oxide particle preparation was carried out by applying the co-precipitation method, outlined as follows: 13 g of Zn  $(\text{CH}_3\text{COO})_2 \cdot 2\text{H}_2\text{O}$  was dissolved in 100 mL MeOH under constant stirring for 2 h. at a temperature of 80 °C, and a transparent solution was formed. Then, the pH was adjusted in the range of 9–11 using 5 mL of  $\text{NH}_4\text{OH}$ . After the solution was dried at 100 °C for 1 h, the temperature was raised to 150 °C to allow solvent evaporation and formation of white precipitation gelatin. The white precipitate was filtrated, washed several times with double-distilled water, and finally rinsed using absolute alcohol. The filtrated product was dried at 200 °C and then calcined at 500 °C in an air atmosphere for 3 h. The result was N-ZnO materials.

### 2.3. Synthesis of Nano-Copper Oxides

Similarly, the method of co-precipitation was utilized to synthesize N-copper oxide particles. The process of synthesis included dissolving 2.5 g of Cu  $(\text{CH}_3\text{COO}) \cdot \text{H}_2\text{O}$  in 20 mL MeOH under vigorous stirring for 1 h. At a temperature of 60 °C, it led to the formation of copper (II) hydroxide powder,  $\text{Cu}(\text{OH})_2$ . The powder was sintered at a temperature of 300 °C for 1 h. Finally, the temperature was raised to 700 °C, which resulted in a black powder of N-CuO.

### 2.4. Preparation of Frac Fluid

Frac fluid was prepared using the water-based Frac system with 0.5% percentages of additives at a laboratory scale with several sequential steps. Initially, one liter of distilled water was taken in the blender and the additives were added. First, 40 g of potassium chloride (KCl) was added to create a brine carrier, and 4.2 g of pure guar gum was added to thicken the water to suspend the proppant. Then, 1 mL of surfactant (Tween or NP9) was added to increase the frac fluid's viscosity, reaching 350 cp. The pH value was recorded as 7.5. After that, different concentrations of nanomaterials were added, including 0.5 g of CNTs, 10 g of N-CuO, and 1 g of N-ZnO. These materials were selected for the study from the previous survey studies [16,30,31]. Then, 4 mL of the breaker (ammonium persulfate) and 3 mL of crosslinker (borax) were added at concentrations of 50 g/100 mL and 5 g/100 mL, respectively. Finally, 4 mL of sodium hydroxide (NaOH) was added to adjust the pH value to 9.5, resulting in the production of a crosslinked fracturing fluid gel with high viscosity. This gel is used to simulate hydraulic fracturing under the high-pressure and high-temperature conditions found in oil reservoirs. Figure 3 illustrates the flow diagram of the frac fluid compounds that were utilized in the preparation process.

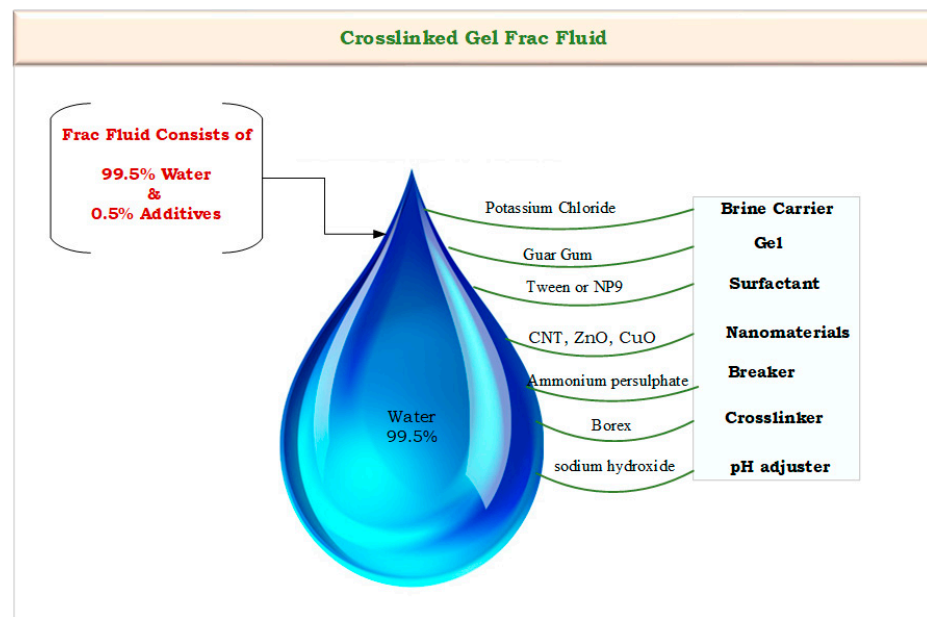


**Figure 3.** Flow diagram of the frac fluid compounds.

### 2.5. Characterizations

In this study, the nanoparticles deemed for the frac fluid preparation were CNTs, N-ZnO, and N-CuO, which were effectively synthesized by the precipitation method. Characterization of CNTs, N-ZnO, and N-CuO particles was ascertained by high-resolution transmission electron microscopy (HR-TEM) and dynamic light scattering (DLS) analysis. All the experiments were conducted at the Egyptian Petroleum Research Institute.

#### 2.5.1. HR-Transmission Electron Microscope

The high-resolution transmission electron microscopy (HR-TEM) technique uses an electron beam to capture images of nanoparticle samples such as CNTs, N-ZnO, and N-CuO. This method provides a much higher resolution than light-based imaging techniques and is preferred for measuring the size of nanoparticles, grain size, size distribution, and material morphology. A HR\_TEM JEM-2100 from JEOL, Japan was used, providing a scale of up to 200 nm, 200 KV voltage, and magnification scale of  $X 15 \times 10^5$ . To prepare the samples for TEM research, the nanoparticles were placed on carbon-coated TEM grids, and the film on the grid was dried before analysis. The utilization of carbon-coated TEM grids ensures the stability of the samples for analysis under the electron beam. TEM imaging is a crucial tool in materials science research, as it enables scientists to study properties at the atomic level and nanoparticle characteristics. Additionally, the capabilities of the HR\_TEM JEM-2100 allow observation of crystalline structures and the surface morphology of nanoparticles with extraordinary clarity. This level of detail is vital for understanding the behavior and interactions of nanoparticles in various environments, especially in oil and gas industrial applications. TEM imaging, in combination with other analytical techniques, can help researchers gain a comprehensive estimation of the composition and behavior of nanoparticles, leading to improvements in fields such as nanotechnology, catalysis, and environmental sciences. The ability to visualize nanoparticles at the atomic level opens up a world of possibilities for designing and engineering materials with tailored properties and functionalities [34–36]. The resolving power of HR-TEM is determined by the wavelength of the electrons used, which can be calculated using the de Broglie wavelength equation:

$$\lambda = \frac{h}{p} \quad (1)$$

where:

$\lambda$  is the de Broglie wavelength (meters).

$h$  is Planck's constant ( $6.626 \times 10^{-34} \text{ m}^2 \text{ kg/s}$ ).

$P$  is the momentum of the electrons ( $\text{kg m/s}$ ).

The momentum of an electron can be expressed as:

$$p = m \cdot v \quad (2)$$

where:

$m$  is the mass of the electron ( $9.109 \times 10^{-31} \text{ kg}$ ).

$v$  is the velocity of the electron ( $\text{m/s}$ ).

Substituting the expression for momentum  $p$  into the de Broglie wavelength equation obtains:

$$\lambda = \frac{h}{m \cdot v} \quad (3)$$

The equation employed in high-resolution transmission electron microscopy (HR-TEM) is utilized to compute the de Broglie wavelength of the electrons traversing the sample. This calculation aids in determining the attainable resolution of the microscope [37].

### 2.5.2. Dynamic Light Scattering (DLS)

A widely used method for measuring particle size is dynamic light scattering (DLS), also known as photon-correlation spectroscopy (PCS). The Zetasizer (Nano-ZS), Malven, UK, is a popular tool for conducting DLS measurements. By analyzing changes in particle size, one can determine the size distribution and understand its motion in the medium. This is achieved by calculating the diffusion coefficient and analyzing the autocorrelation function [38]. DLS is particularly beneficial for nanoparticle investigation, colloids, and proteins in solution. The Zetasizer (Nano-ZS) employs laser technology to measure the fluctuations in light scattering caused by Brownian motion of particles. By accurately measuring particle size and distribution, researchers can gain valuable insights into the behavior and stability of colloidal systems [39].

The DLS analysis equation is utilized to examine the size distribution of particles in a sample by assessing the variations in the intensity of scattered light. The primary equation employed in dynamic light scattering (DLS) analysis is the Stokes–Einstein equation [40]. This equation establishes a relationship between the diffusion coefficient ( $D$ ), particle radius ( $a$ ), temperature ( $T$ ), viscosity ( $\eta$ ), and Boltzmann's constant ( $k$ ), as follows:

$$D = \frac{k \cdot T}{6 \cdot \pi \cdot \eta \cdot a} \quad (4)$$

where:

$D$  is the diffusion coefficient.

$k$  is Boltzmann's constant ( $1.38 \times 10^{-23} \text{ m}^2 \cdot \text{kg} \cdot \text{s}^{-2} \cdot \text{K}^{-1}$ ).

$T$  is the absolute temperature in Kelvin.

$\eta$  is the viscosity of the solvent in  $\text{kg} \cdot \text{m}^{-1} \cdot \text{s}^{-1}$ .

$a$  is the particle radius.

### 2.6. Frac Fluid Rheology Test

The study of the deformation and flow behavior of various materials is known as rheology, while rheometer refers to the experimental techniques and tools used to determine rheological properties. Viscosity can be determined by measuring the resistance of a sample as it is sheared. Emphasizing the rheological properties of the frac fluid sample is essential in determining the behavior and suitability for various applications. It has been observed that the viscosity of the sample decreases with an increase in temperature, indicating the significant influence of temperature on its rheological properties. Therefore, it is crucial to carefully consider and control the temperature conditions during the testing and application

of the sample to ensure optimal performance and desired outcomes [41]. Rheological experiments were conducted using the Anton Paar MCR 502 rheometer, Montreal, Canada, wherein the apparent viscosity measurements were obtained by varying the shear rate or time at different temperatures according to Equation (5), which shows the relation of the ratio of the shear stress to shear rate to determine the viscosity to evaluate the rheological properties. It was observed that allowing a period of 1 min before measurement was necessary to attain equilibrium in the system and avoid complexities related to time-dependent phenomena associated with gel rheology [42].

$$\eta = \tau \div \gamma \quad (5)$$

where:

$\eta$  is viscosity,  $\tau$  is shear stress, and  $\gamma$  is shear rate.

### 3. Results and Discussion

#### 3.1. Characterization of Nanomaterials

High-resolution transmission electron microscopy (HR-TEM) and dynamic light scattering (DLS) analysis were conducted to investigate the effect of the precursor concentration, temperature, and time of growth on the structure grain size during the synthesis and characterization of CNTs, N-ZnO, and N-CuO.

##### 3.1.1. HR-TEM Analysis

Figure 4 shows the HR-TEM image of nanomaterials CNTs, N-ZnO, and N-CuO with distribution scales of 50 nm, 100 nm, and 200 nm, voltage of 200 Kv, and magnification of  $X50 \times 10^3$ ,  $X25 \times 10^3$ , and  $X20 \times 10^3$ , using HR-TEM. The HR-TEM image shown in Figure 4A reveals that CNTs are multi-walled nanotubes with diameters ranging from 10–500 nm. Additionally, the N-ZnO image in (Figure 4B) demonstrates that nanoparticles possess a spherical and longitudinal spherical shape with narrow dispersion. In the same manner, Figure 4C illustrates the N-CuO grain distribution, characterized by a narrow and heterogenic morphological appearance, including spherical and rod-shaped N-CuO.

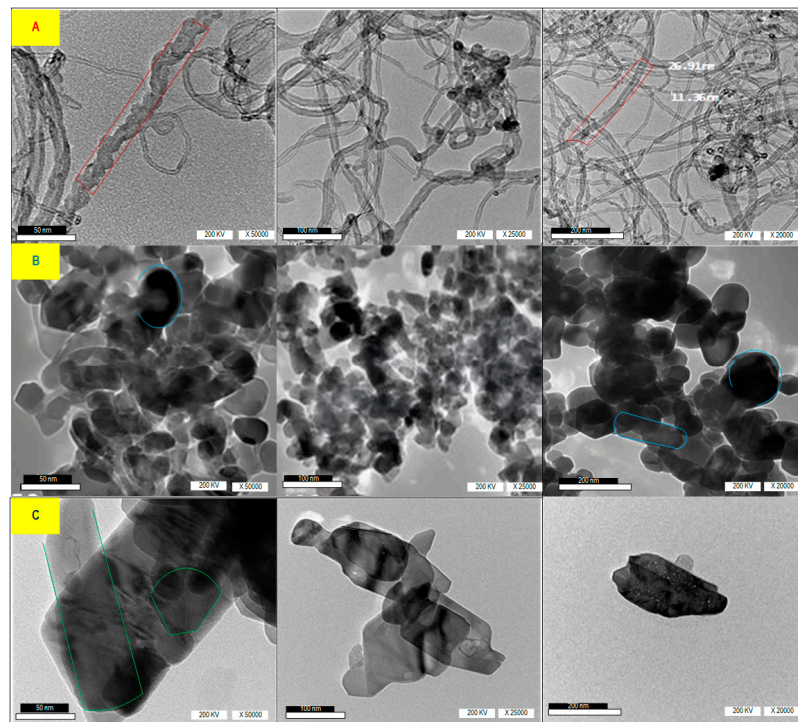


**Figure 4.** HR-TEM image of (A) CNTs, (B) N-ZnO, and (C) N-CuO with distribution scales of 50 nm, 100 nm, and 200 nm.

The shape and distribution of nanoparticles play a crucial role in the rheological behavior of frac fluid and its ability to withstand pressure and temperature in the reservoir. Although the three materials of CNTs, N-ZnO, and N-CuO have narrow dispersion, CNTs with long tube shapes help maintain the high viscosity of frac fluid for a long duration. In contrast, weak crosslinking between frac fluid molecules results in less resistance to temperature. Therefore, CNTs are more beneficial for improving rheological properties compared to N-ZnO and N-CuO. Additionally, the long tube shapes of CNTs provide more surface area for interaction with other molecules in the frac fluid, enhancing its stability and overall performance. On the other hand, the narrow dispersion of N-ZnO and N-CuO may limit their effectiveness in improving the rheological properties of frac fluid. Overall, the unique shape and distribution of nanoparticles, particularly CNTs, can significantly impact the ability of frac fluid to maintain viscosity and withstand challenging reservoir conditions.

### 3.1.2. DLS Analysis

Figure 5 represents the DLS of N-ZnO and N-CuO particles. DLS analysis is employed to quantify the nanomaterial particle size depending on the z average, intensity, and particle numbers indicating the poly disparity index (PDX). The PDX is mostly less than 0.6 (Ref). Accordingly, the CNT particle distribution is very narrow, with a PDX equal to 0.4, and the CNT diameter ranges between 10 nm and 500 nm, resulting from TEM analysis. Similarly, N-ZnO and N-CuO particle distribution is very narrow, with a PDX of 0.3 and 0.4, both less than 0.6, respectively. The z average is approximately 300 nm for N-ZnO and N-CuO, as shown in Figure 5. Table 3 shows the size, mean number, and standard division of DLS analysis of CuO and ZnO nanoparticles. The analysis of nanoparticles using DLS reveals that the average size is around 50 nm, with a deviation of 5 nm. Based on the sample, there are 100 particles on average, indicating a relatively low particle count. Conversely, when analyzing ZnO nanoparticles using DLS, we found a size range of 30–200 nm and an average particle count of 100, with a deviation of 10 nm. The number of nanoparticles for both CuO and ZnO is relatively high, suggesting the presence of particles in the samples. The narrow standard deviation values further support these findings from the PDX analysis, indicating a distribution of particles in both cases.

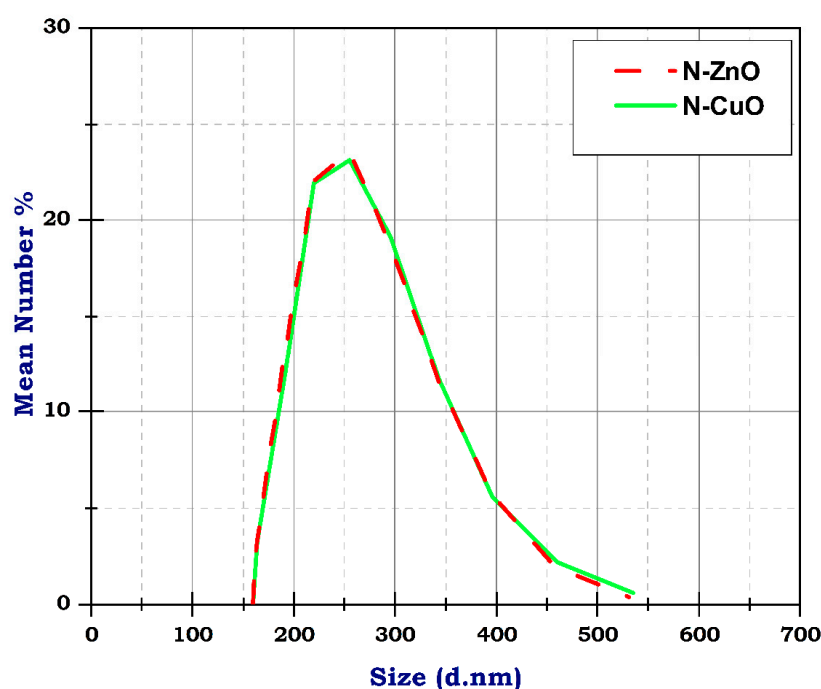


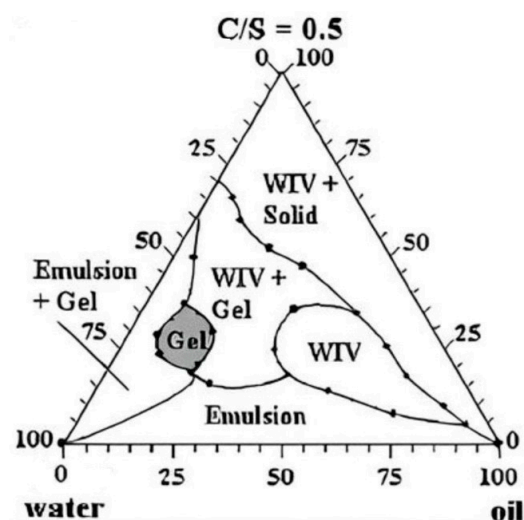
Figure 5. The DLS of N-ZnO and N-CuO particles.

**Table 3.** Size, mean, and standard division of DLS analysis of N-CuO and N-ZnO.

| Materials         | Size (d.nm) | Mean Number % | Standard Division Number % |
|-------------------|-------------|---------------|----------------------------|
| CuO nanoparticles | 164.3       | 3.2           | 0.3                        |
|                   | 192.1       | 12.1          | 1                          |
|                   | 219.7       | 21.9          | 1.1                        |
|                   | 255.0       | 23.1          | 0.5                        |
|                   | 295.3       | 19.1          | 0.3                        |
|                   | 343.5       | 11.7          | 0.8                        |
|                   | 396.5       | 5.6           | 0.9                        |
|                   | 460.2       | 2.2           | 0.6                        |
|                   | 535         | 0.6           | 0.2                        |
| ZnO nanoparticles | 164.2       | 3.3           | 0.3                        |
|                   | 190.1       | 12.7          | 1                          |
|                   | 220.2       | 22            | 1.1                        |
|                   | 255.0       | 23.6          | 0.5                        |
|                   | 295.3       | 18.7          | 0.3                        |
|                   | 342.0       | 11.7          | 0.8                        |
|                   | 396.1       | 5.7           | 0.9                        |
|                   | 458.7       | 1.9           | 0.6                        |
|                   | 531.2       | 0.4           | 0.2                        |

### 3.2. Rheological Measurements of Frac Fluid

Frac fluid is vital in hydraulic fracturing treatment to carry and transport proppants into the fracture. Specifically, the water-based frac fluids are prepared successfully at the laboratory scale with highly viscous borate-crosslinked gels with different concentrations of nanomaterials (CNTs, N-ZnO, and N-CuO) to apply in oil wells with high pressure and high temperatures. On the other hand, the pseudo-ternary phase diagram was constructed to identify the gel region, illustrated in Figure 6. The aim of studying the gel strength effects alongside buffers is to prevent the pH from falling and causing the polymer to break down.

**Figure 6.** Pseudo-ternary diagram showing the gel region of the fracturing fluid [43].

The apparent viscosity was measured by changing the shear rate or time at different temperatures. Table 4 summarizes the viscosity measurements of the prepared frac fluid

conducted at various temperatures and constant shear stress for 3 min. By interpreting the data in the table and referring to Figures 7–11, the examination of the fracturing fluid samples with the utilization of nanomaterials in the preparation and the blank sample is presented.

**Table 4.** Viscosity of prepared frac fluids with or without nanomaterials.

| Temperature | The Viscosity of Frac Fluid (cp) |       |       |       |
|-------------|----------------------------------|-------|-------|-------|
|             | CNTs                             | N-ZnO | N-CuO | Blank |
| 25          | 550                              | 206   | 206   | 163   |
| 30          | 500                              | 160   | 155   | 124   |
| 35          | 472                              | 121   | 120   | 100   |
| 40          | 445                              | 65    | 60    | 50    |
| 45          | 370                              | 24    | 24    | 20    |
| 50          | 360                              | 17    | 16    | 10    |

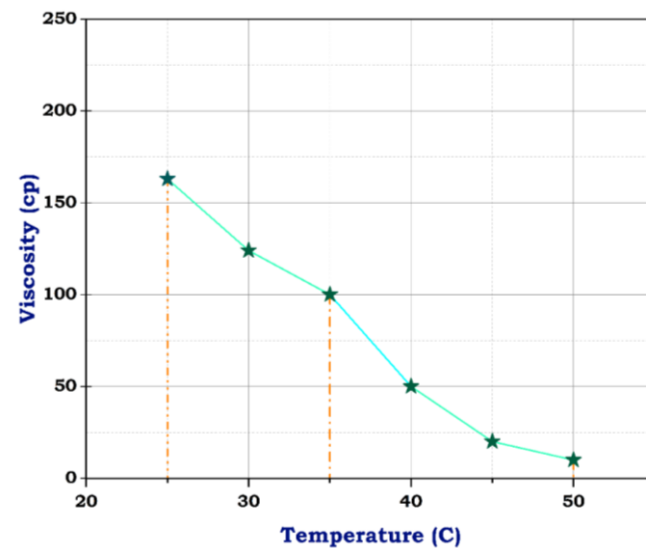


**Figure 7.** Viscosity of blank frac fluid.

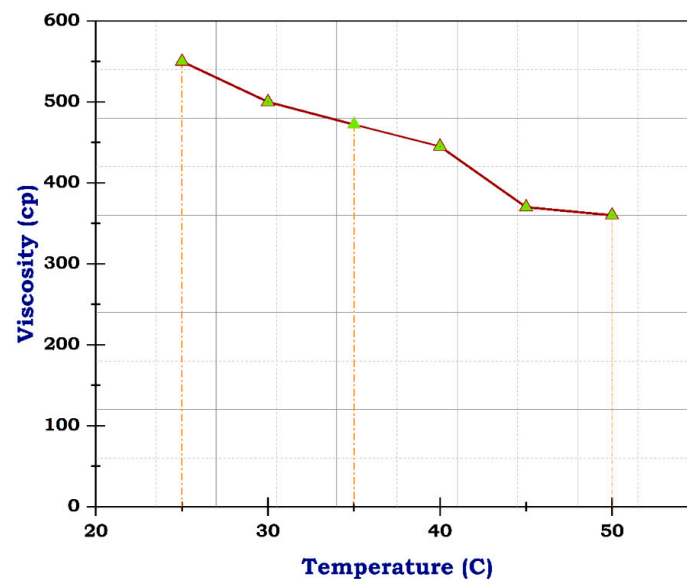


**Figure 8.** Viscosity of frac fluid with CNTs.

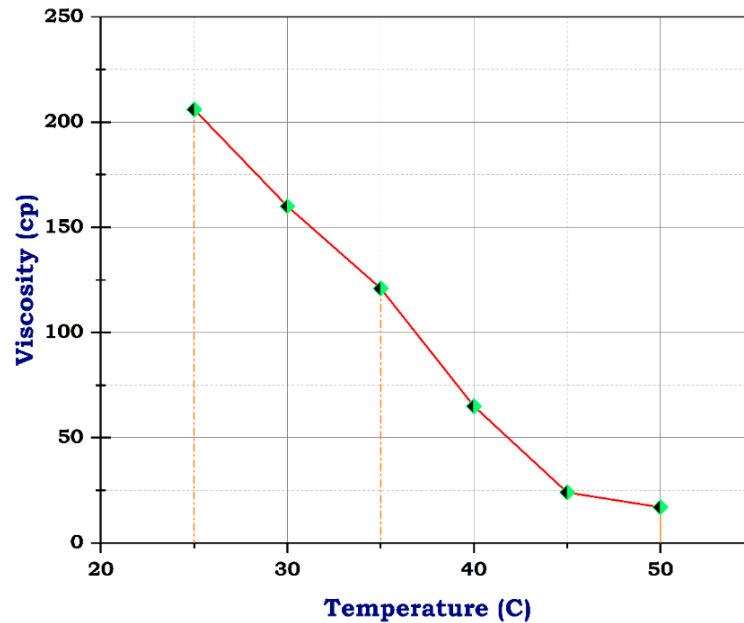


Figure 9. Viscosity of frac fluid with N-ZnO.

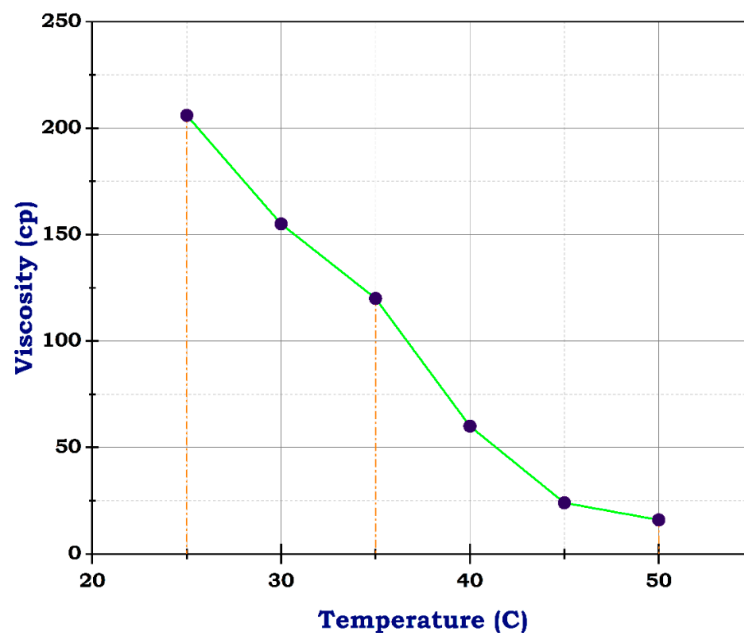


Figure 10. Viscosity of frac fluid with N-CuO.

The viscosity of blank frac fluid before adding any of the nanomaterials under a temperature of 25 °C was only 163 cp, and rose to less than 100 cp at a temperature between 35 °C and 40 °C by the end of the rheological test; the viscosity dropped to 10 cp when the temperature reached 50 °C, as illustrated in Figure 7. This significant decrease in viscosity as the temperature rises suggests a high-temperature sensitivity of the blank frac fluid. This rapid decline in viscosity may impact the fluid's effectiveness in downhole conditions, especially at elevated temperatures. Therefore, the addition of nanomaterials could potentially help stabilize the viscosity of the fluid at higher temperatures, preventing it from dropping too low. Fortunately, utilizing carbon nanotubes has advantages due to their structure and resistance to temperature. Although the concentration of CNTs was 0.5 g, the viscosity of frac fluid prepared with CNTs was 550 cp at 25 °C, then reached 360 cp on finishing the analysis, likely with acceptable drop-down, illustrated in Figure 8. The use of carbon nanotubes significantly improved the viscosity of the fracturing fluid compared

to the fluid without CNTs. Despite the relatively low concentration of CNTs, the viscosity remained consistently high throughout the rheological test. This indicates that including carbon nanotubes in the fluid formulation offers enhanced resistance to temperature changes, resulting in improved overall performance. The stable viscosity achieved through the incorporation of CNTs suggests that the fluid can efficiently transport proppants into fractures without experiencing significant viscosity reduction. This is essential for ensuring successful fracturing operations and optimizing oil and gas production. Therefore, these results demonstrate the potential of employing carbon nanotubes in fracturing fluids to achieve improved efficiency and effectiveness in hydraulic fracturing operations.

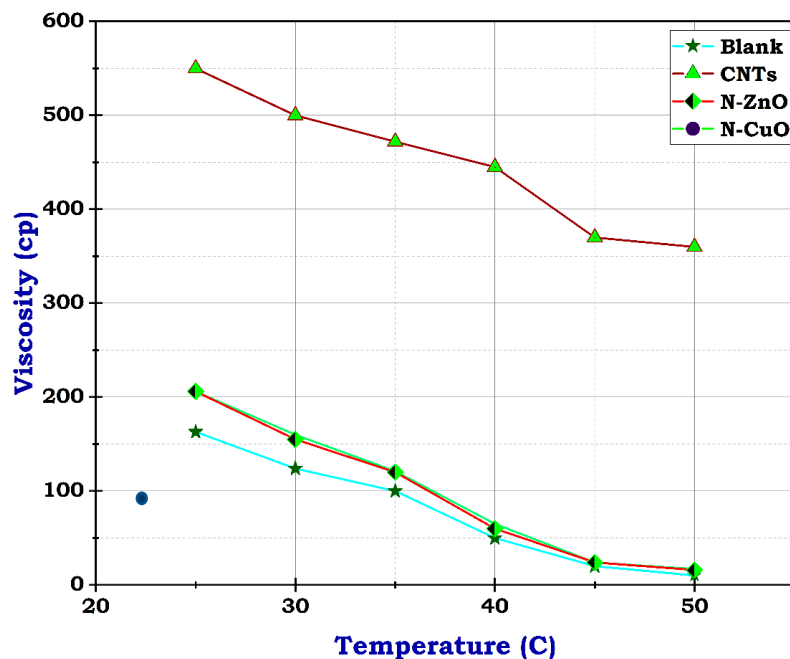


Figure 11. Viscosity of the prepared frac fluids.

Unlikely, the sample with CuO and ZnO nanoparticles had 206 cp at 25 °C, almost its viscosity near that of the blank sample at concentrations of 10 g and 1 g, respectively. At 50 °C, the viscosity dropped to 16 and 17, individually, as shown in Figures 9 and 10. These results suggest that the addition of CuO and ZnO nanoparticles has a significant effect on the viscosity of the sample, especially at higher temperatures. The decrease in viscosity indicates that the nanoparticles may facilitate better flow and reduce resistance within the sample. These findings could have important implications for various industries, such as materials science and manufacturing, where controlling viscosity is crucial for optimizing performance. Therefore, this study shows promising potential for utilizing N-CuO and N-ZnO nanoparticles to augment the flow characteristics of materials at higher temperatures. The potential viscosity reduction afforded by these nanoparticles holds the promise of enhancing processing efficiency and product quality across various applications. Further research is needed to understand the mechanisms behind this phenomenon fully and to determine the optimal concentrations of nanoparticles, especially for oil and gas production enhancement.

To sum up, referring to the reference test of the blank sample viscosity readings, the results revealed that adding CNTs improves the gel strength by 337.4% and 126.4% for N-ZnO and N-CuO, respectively. Increasing the temperature resulted in the reduction of frac fluid viscosity readings. The gel strength decreased significantly, reaching 10.4% and 9.8% for N-ZnO and N-CuO, respectively. Otherwise, CNTs showed more resistance, reaching 220.9%, indicating that the blank sample improved the viscosity and kept the fluid more stable by keeping the gel strength and crosslinking within fluids under high-pressure and high-temperature reservoir conditions. Thus, utilizing CNTs improves the rheological

properties of fluid better than N-ZnO and N-CuO. Furthermore, those findings suggest that CNTs are the most effective additive for enhancing the rheological properties of frac fluid, with a significant increase in gel strength and viscosity in the presence of CNTs even under high-pressure and high-temperature reservoir conditions. In contrast, N-ZnO and N-CuO showed lower effectiveness in improving fluid stability. This indicates that CNTs are a more suitable additive for boosting the performance of frac fluids in hydraulic fracturing operations. Further research and testing could further refine the utilization of CNTs in frac fluid formulations to achieve optimal efficiency.

#### 4. Conclusions and Recommendations

This study focused on investigating the effect of utilizing nanomaterials to improve the rheological properties of frac fluids for enhancing oil reservoir production. The Delta Frac system was applied, in addition to using materials of CNTs, N-ZnO, and N-CuO with concentrations of 0.5 g, 1 g, and 10 g per 1 L of water, respectively. The result showed that nano-size ranges were 10–500 nm, 300 nm, and 295 nm for CNTs, N-ZnO, and N-CuO, respectively. The utilization of carbon nanotubes demonstrated promising results, with a resistance of 550 cp at 25 °C and reached 360 cp at 50 °C despite the low concentration of 0.5 g/L utilized in the fluid. On the other hand, using N-CuO and N-ZnO showed initial resistance of 206 cp at 25 °C, which then significantly decreased to 17 cp and 16 cp, respectively, with higher concentrations of 10 g/L and 1 g/L. Therefore, utilizing CNTs or carbon nanomaterials sourced from plastic waste materials to reduce costs and promote environmental sustainability is highly recommended. These nanomaterials not only possess unique physical and chemical properties but also have the potential to enhance oil reservoir production.

**Author Contributions:** Conceptualization, F.Y., W.G. and K.I.K.; methodology, F.Y., W.G., A.G.A.-G. and C.Y.; validation, C.Y., L.L. and K.I.K.; formal analysis, F.Y., W.G. and A.G.A.-G.; investigation, F.Y., W.G. and A.G.A.-G.; resources, K.I.K. and L.L.; data curation, F.Y. and W.G.; writing—original draft preparation, F.Y.; writing—review and editing, W.G., A.G.A.-G., N. and C.Y.; visualization, F.Y.; supervision, K.I.K. and L.L. All authors have read and agreed to the published version of the manuscript.

**Funding:** Alliance of International Science Organizations (ANSO) at the University of Science and Technology of China (USTC) funded through the ANSO Scholarship for Young Talents. Academy of Scientific Research and Technology (ASRT) under the Egyptian Ministry of Higher Education, Egypt, funded through the program of Scientists for Next Generation (SNG).

**Data Availability Statement:** Data are contained within the article.

**Conflicts of Interest:** The authors state that they do not have any competing financial interests or personal relationships that could have influenced the work reported in this paper.

#### References

1. Barati, R.; Liang, J.T. A review of fracturing fluid systems used for hydraulic fracturing of oil and gas wells. *J. Appl. Polym. Sci.* **2014**, *131*, 1–11. [[CrossRef](#)]
2. Rahm, D. Regulating hydraulic fracturing in shale gas plays: The case of Texas. *Energy Policy* **2011**, *39*, 2974–2981. [[CrossRef](#)]
3. Thomas, L.; Tang, H.; Kalyon, D.M.; Aktas, S.; Arthur, J.D.; Blotvogel, J.; Carey, J.W.; Filshill, A.; Fu, P.; Hsuan, G.; et al. Toward better hydraulic fracturing fluids and their application in energy production: A review of sustainable technologies and reduction of potential environmental impacts. *J. Pet. Sci. Eng.* **2019**, *173*, 793–803. [[CrossRef](#)]
4. Hurnaas, T.; Plank, J. Behavior of Titania Nanoparticles in Cross-linking Hydroxypropyl Guar Used in Hydraulic Fracturing Fluids for Oil Recovery. *Energy Fuels* **2015**, *29*, 3601–3608. [[CrossRef](#)]
5. Liu, J.; Sheng, J.J.; Emadibaladehi, H.; Tu, J. Experimental study of the stimulating mechanism of shut-in after hydraulic fracturing in unconventional oil reservoirs. *Fuel* **2021**, *300*, 120982. [[CrossRef](#)]
6. Huang, Q.; Liu, S.; Wang, G.; Cheng, W. Evaluating the changes of sorption and diffusion behaviors of Illinois coal with various water-based fracturing fluid treatments. *Fuel* **2021**, *283*, 118884. [[CrossRef](#)]
7. Montgomery, C. Fracturing fluids. In Proceedings of the ISRM International Conference for Effective and Sustainable Hydraulic Fracturing, Brisbane, Australia, 20–22 May 2013; OnePetro: Richardson, TX, USA, 2013.

8. Wanniarachchi, W.; Ranjith, P.; Perera, M. Shale gas fracturing using foam-based fracturing fluid: A review. *Environ. Earth Sci.* **2017**, *76*, 91. [[CrossRef](#)]
9. Faroughi, S.A.; Pruvot, A.J.-C.J.; McAndrew, J. The rheological behavior of energized fluids and foams with application to hydraulic fracturing: Review. *J. Pet. Sci. Eng.* **2018**, *163*, 243–263. [[CrossRef](#)]
10. Yekeen, N.; Padmanabhan, E.; Idris, A.K. A review of recent advances in foam-based fracturing fluid application in unconventional reservoirs. *J. Ind. Eng. Chem.* **2018**, *66*, 45–71. [[CrossRef](#)]
11. Yehia, S.T.F.; Noah, A.Z.; Abou Heleik, M.M.; Kabel, K.I. Hydraulic Fracturing Process Systems and Fluids: An Overview. *Pet. Petrochem. Eng. J.* **2022**, *6*, 000306. [[CrossRef](#)]
12. Daneshfar, R.; Mohammadzadeh, H.; Kamranfar, P.; Shahbazi, K. Hydraulic Fracturing Fluids: A Comprehensive Review Focusing on Nanoparticle-Enhanced Fluids. In Proceedings of the National Conference of Fundamental and Engineering Sciences, Schaumburg, IL, USA, 13–15 October 2017.
13. Khalil, M.; Jan, B.M.; Tong, C.W.; Berawi, M.A. Advanced nanomaterials in oil and gas industry: Design, application and challenges. *Appl. Energy* **2017**, *191*, 287–310. [[CrossRef](#)]
14. Li, W.; Liu, J.; Zeng, J.; Tian, J.; Li, L.; Zhang, M.; Jia, J.; Li, Y.; Peng, H.; Zhao, X. A critical review of the application of nanomaterials in frac fluids: The state of the art and challenges. In Proceedings of the SPE Middle East Oil and Gas Show and Conference, Manama, Bahrain, 18–21 March 2019; OnePetro: Richardson, TX, USA, 2019.
15. Boul, P.J.; Ajayan, P.M. Nanotechnology research and development in upstream oil and gas. *Energy Technol.* **2020**, *8*, 1901216. [[CrossRef](#)]
16. Liu, J.; Wang, S.; Wang, C.; Zhao, F.; Lei, S.; Yi, H.; Guo, J. Influence of nanomaterial morphology of guar-gum fracturing fluid, physical and mechanical properties. *Carbohydr. Polym.* **2020**, *234*, 115915. [[CrossRef](#)] [[PubMed](#)]
17. Li, L.; Al-Muntasheri, G.A.; Liang, F. Nanomaterials-enhanced high-temperature fracturing fluids prepared with untreated seawater. In Proceedings of the SPE Annual Technical Conference and Exhibition, Dubai, United Arab Emirates, 26–28 September 2016; OnePetro: Richardson, TX, USA, 2016.
18. Zhou, B.; You, Q.; Li, Y.; Chu, Z.; Zhang, L.; Wang, P.; Liu, C.; Dai, C. Preparation and performance evaluation of an active nanofluid for enhanced oil recovery in ultra-low permeability reservoirs. *J. Mol. Liq.* **2022**, *347*, 118331. [[CrossRef](#)]
19. Liu, C.; Li, Y.; Wang, P.; Jiao, H.; Yao, X.; Zhao, G.; Dai, C.; You, Q. Preparation and performance evaluation of nano-composite fracturing fluid with good oil displacement ability in tight reservoir. *J. Mol. Liq.* **2022**, *367*, 120494. [[CrossRef](#)]
20. Mao, Z.; Cheng, L.; Liu, D.; Li, T.; Zhao, J.; Yang, Q. Nanomaterials and technology applications for hydraulic fracturing of unconventional oil and gas reservoirs: A state-of-the-art review of recent advances and perspectives. *ACS Omega* **2022**, *7*, 29543–29570. [[CrossRef](#)] [[PubMed](#)]
21. Abid, N.; Khan, A.M.; Shujait, S.; Chaudhary, K.; Ikram, M.; Imran, M.; Haider, J.; Khan, M.; Khan, Q.; Maqbool, M. Synthesis of nanomaterials using various top-down and bottom-up approaches, influencing factors, advantages, and disadvantages: A review. *Adv. Colloid Interface Sci.* **2022**, *300*, 102597. [[CrossRef](#)] [[PubMed](#)]
22. Vaseghi, Z.; Nematollahzadeh, A. Nanomaterials: Types, synthesis, and characterization. In *Green Synthesis of Nanomaterials for Bioenergy Applications*; Wiley: Hoboken, NJ, USA, 2020; pp. 23–82.
23. Kolahalam, L.A.; Viswanath, I.K.; Diwakar, B.S.; Govindh, B.; Reddy, V.; Murthy, Y. Review on nanomaterials: Synthesis and applications. *Mater. Today Proc.* **2019**, *18*, 2182–2190. [[CrossRef](#)]
24. Li, H.; Yang, B.-S. Model evaluation of particle breakage facilitated process intensification for Mixed-Suspension-Mixed-Product-Removal (MSMPR) crystallization. *Chem. Eng. Sci.* **2019**, *207*, 1175–1186. [[CrossRef](#)]
25. Adam, R.E.; Pozina, G.; Willander, M.; Nur, O. Synthesis of ZnO nanoparticles by co-precipitation method for solar driven photodegradation of Congo red dye at different pH. *Photonics Nanostruct.-Fundam. Appl.* **2018**, *32*, 11–18. [[CrossRef](#)]
26. Phiw dang, K.; Suphankij, S.; Mekprasart, W.; Pecharapa, W. Synthesis of CuO nanoparticles by precipitation method using different precursors. *Energy Procedia* **2013**, *34*, 740–745. [[CrossRef](#)]
27. Ghorbani, H.R.; Mehr, F.P.; Pazoki, H.; Rahmani, B.M. Synthesis of ZnO nanoparticles by precipitation method. *Orient. J. Chem.* **2015**, *31*, 1219–1221. [[CrossRef](#)]
28. Tang, W.; Zou, C.; Peng, H.; Wang, Y.; Shi, L. Influence of nanoparticles and surfactants on stability and rheological behavior of polymeric nanofluids and the potential applications in fracturing fluids. *Energy Fuels* **2021**, *35*, 8657–8671. [[CrossRef](#)]
29. Ismail, A.; Aftab, A.; Ibupoto, Z.; Zolkifile, N. The novel approach for the enhancement of rheological properties of water-based drilling fluids by using multi-walled carbon nanotube, nanosilica and glass beads. *J. Pet. Sci. Eng.* **2016**, *139*, 264–275. [[CrossRef](#)]
30. Alkalbani, A.M.; Chala, G.T.; Zar Myint, M.T. Insightful study on the effect of zinc oxide nanoparticle diameter on the rheology of water base mud at elevated temperature. *J. Pet. Sci. Eng.* **2022**, *217*, 110878. [[CrossRef](#)]
31. Ahmed Mansoor, H.H.; Devarapu, S.R.; Samuel, R.; Sangwai, J.S.; Ponmani, S. Investigation of chia based copper oxide nanofluid for water based drilling fluid: An experimental approach. *J. Nat. Gas Sci. Eng.* **2022**, *107*, 104775. [[CrossRef](#)]
32. William, J.K.M.; Ponmani, S.; Samuel, R.; Nagarajan, R.; Sangwai, J.S. Effect of CuO and ZnO nanofluids in xanthan gum on thermal, electrical and high pressure rheology of water-based drilling fluids. *J. Pet. Sci. Eng.* **2014**, *117*, 15–27. [[CrossRef](#)]
33. Al-saba, M.T.; Al Fadhli, A.; Marafi, A.; Hussain, A.; Bander, F.; Al Dushaishi, M.F. Application of Nanoparticles in Improving Rheological Properties of Water Based Drilling Fluids. In Proceedings of the SPE Kingdom of Saudi Arabia Annual Technical Symposium and Exhibition, Dammam, Saudi Arabia, 23–26 April 2018.

34. Franken, L.E.; Grünewald, K.; Boekema, E.J.; Stuart, M.C. A Technical Introduction to Transmission Electron Microscopy for Soft-Matter: Imaging, Possibilities, Choices, and Technical Developments. *Small* **2020**, *16*, 1906198. [[CrossRef](#)]
35. Govender, K.; Boyle, D.S.; Kenway, P.B.; O'Brien, P. Understanding the factors that govern the deposition and morphology of thin films of ZnO from aqueous solution. *J. Mater. Chem.* **2004**, *14*, 2575–2591. [[CrossRef](#)]
36. Nath, D.; Singh, F.; Das, R. X-ray diffraction analysis by Williamson-Hall, Halder-Wagner and size-strain plot methods of CdSe nanoparticles—a comparative study. *Mater. Chem. Phys.* **2020**, *239*, 122021. [[CrossRef](#)]
37. Reimer, L. *Transmission Electron Microscopy: Physics of Image Formation and Microanalysis*; Springer: Berlin/Heidelberg, Germany, 2013; Volume 36.
38. Priya, M.; Premkumar, V.K.; Vasantharani, P.; Sivakumar, G. Structural and electrochemical properties of ZnCo<sub>2</sub>O<sub>4</sub> nanoparticles synthesized by hydrothermal method. *Vacuum* **2019**, *167*, 307–312. [[CrossRef](#)]
39. Filippov, S.K.; Khusnutdinov, R.; Murmiliuk, A.; Inam, W.; Zakharova, L.Y.; Zhang, H.; Khutoryanskiy, V.V. Dynamic light scattering and transmission electron microscopy in drug delivery: A roadmap for correct characterization of nanoparticles and interpretation of results. *Mater. Horiz.* **2023**, *10*, 5354–5370. [[CrossRef](#)]
40. Berne, B.J.; Pecora, R. *Dynamic Light Scattering: With Applications to Chemistry, Biology, and Physics*; Courier Corporation: Chelmsford, MA, USA, 2000.
41. Bhattad, A.; Atgur, V.; Rao, B.N.; Banapurmath, N.; Yunus Khan, T.; Vadlamudi, C.; Krishnappa, S.; Sajjan, A.; Shankara, R.P.; Ayachit, N. Review on Mono and Hybrid Nanofluids: Preparation, Properties, Investigation, and Applications in IC Engines and Heat Transfer. *Energies* **2023**, *16*, 3189. [[CrossRef](#)]
42. Mercan, H. Chapter 3—Thermophysical and rheological properties of hybrid nanofluids. In *Hybrid Nanofluids for Convection Heat Transfer*; Ali, H.M., Ed.; Academic Press: Cambridge, MA, USA, 2020; pp. 101–142.
43. Santanna, V.C.; de Castro Dantas, T.N.; Neto, A.A.D. The Use of Microemulsion Systems in Oil Industry. In *Microemulsions: An Introduction to Properties and Applications*; IntechOpen: London, UK, 2012; pp. 161–174.

**Disclaimer/Publisher's Note:** The statements, opinions and data contained in all publications are solely those of the individual author(s) and contributor(s) and not of MDPI and/or the editor(s). MDPI and/or the editor(s) disclaim responsibility for any injury to people or property resulting from any ideas, methods, instructions or products referred to in the content.